Branching Ratio Measurements Of Cluster Structures In $^{18}O^*$

S. Pirrie[1], Tz. Kokalova[1], C. Wheldon[1], J. Bishop[1], R. Hertenberger[2], H.-F. Wirth[2], S. Bailey[1], N. Curtis[1], D. Dell'Aquila[5], Th. Faestermann[3], D. Mengoni[4], R. Smith[1], D. Torresi[1], A. Turner[1]

1. School of Physics and Astronomy, University of Birmingham, B15 2TT
2. Fakultät für Physik, Ludwig-Maximillans-Universität München, D-85748 Garching, Germany
3. Physik Department, Techinische Universität München, D-85748 Garching, Germany
4. Università degli Studi di Padova, Via 8 Febbraio 1848, 2, 35122 Padova PD, Italy
5. Università degli Studi di Napoli Fedorico II, Corso Umberto I, 40, 80138 Napoli NA, Italy

1. Aims and Motivations

- **Rotational bands with cluster structure in ^{18}O** were proposed by von Oertzen *et al.* [1], based on the measurement of **30 previously unobserved states** in an experiment performed using the **Q3D magnetic spectrograph** at the **Maier-Leibnitz Laboratory in Munich**.
- These proposed rotational bands, $K^\pi = 0_2$ and $K^\pi = 0_4$, have **both a negative and positive parity band** associated with them due to **signature splitting**, caused by their asymmetry about the rotation axis.
- The proposed structure of the $K^\pi = 0_2^{+/-}$ bands is a core + α structure of **$^{14}C \otimes \alpha$**.
- The proposed structure of the $K^\pi = 0_4^{+/-}$ bands is a nuclear molecule structure of **$^{12}C \otimes 2n \otimes \alpha$**.
- States with nuclear cluster structure provide an **excellent test of nuclear models** as well as an increased ease in modelling the nuclear system by reduction of its nucleons into clusters.
- Through the **measurement of the branching ratios** for these states through an experiment, **the reduced partial widths** can be determined for each decay mode.
- The **reduced partial α width can be compared with the Wigner limit** to determine the tendency towards clustering, and thus **confirm or refute the proposed bands**.

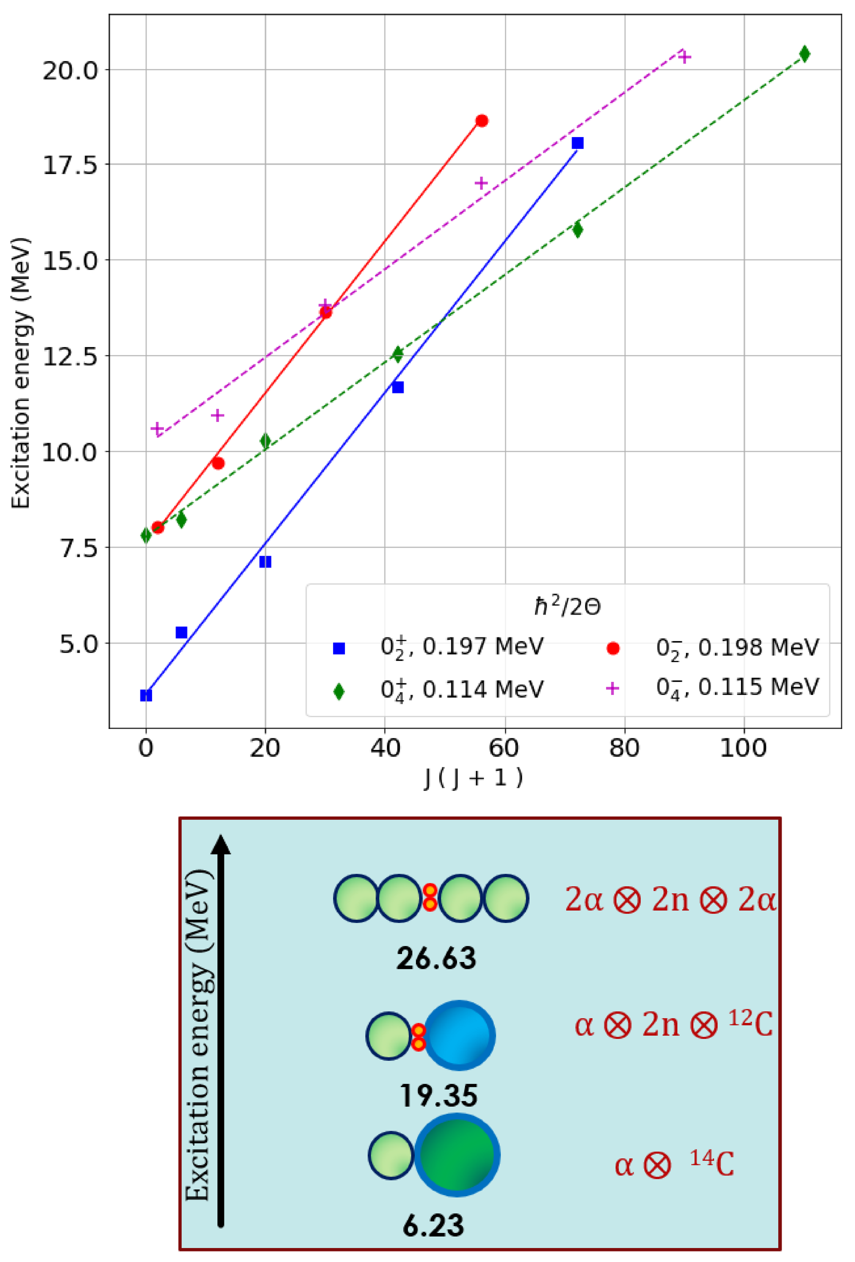

Figure 1: The proposed rotational bands showing the signature splitting (top) and the proposed cluster structures, listed with the energy thresholds at which they can form (bottom).

2. Experimental Set-up

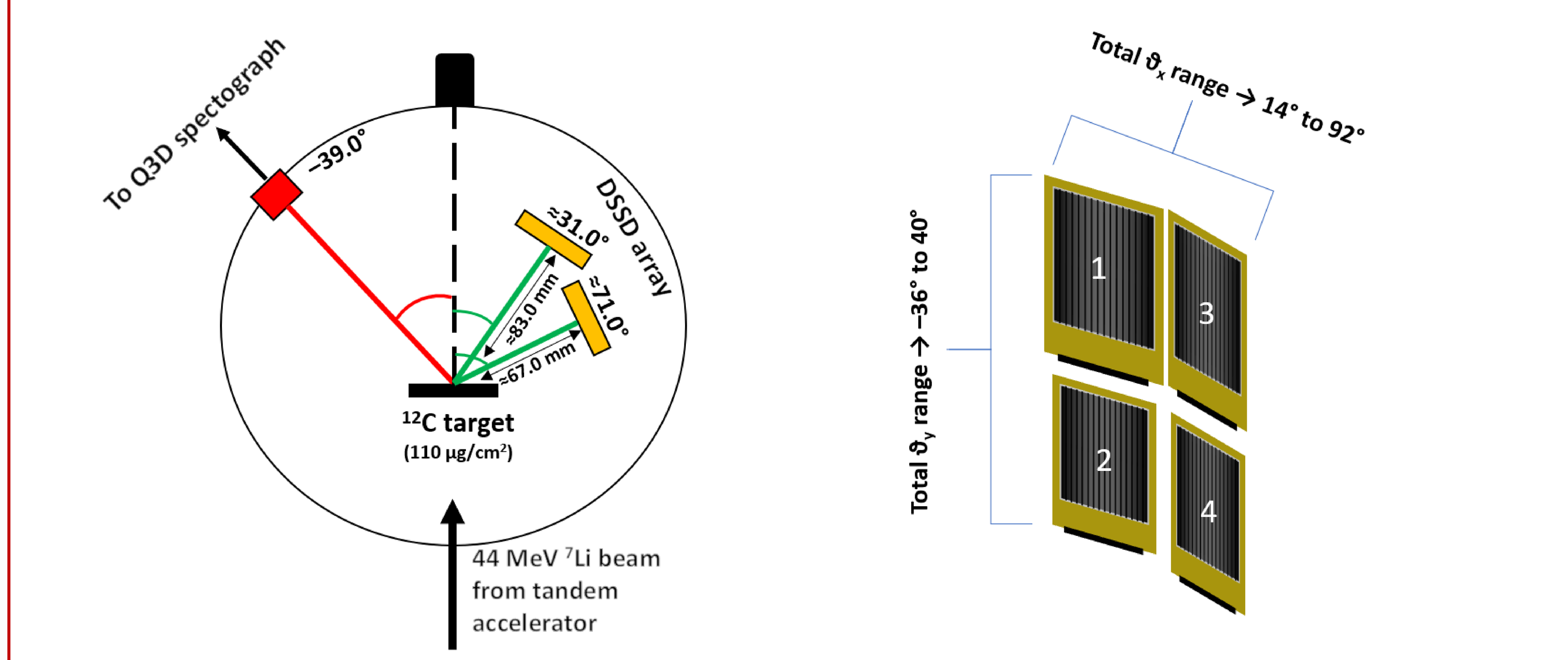

Figure 2: An overview of the experimental set-up used in the experiment (left) and a depiction of the Birmingham DSSD array, showing the total angular coverage (right) [2].

- The experiment was performed, also at the **Maier-Leibnitz Laboratory in Munich**, making use of the **Q3D magnetic spectrograph** [3] in conjunction with the **Birmingham DSSD array** to measure charged particles.
- The reaction that was used to produce ^{18}O in the desired excited states was **$^{12}C(^7Li,p)^{18}O^*$**.
- **The $^{18}O^*$ or its corresponding decay fragments were detected by the DSSD array** to allow for high resolution determination of both their energies and momenta.
- **The proton was detected by the Q3D**, as the particle identification possible through the several stages of the **focal plane detector** contained within the Q3D allowed for events corresponding to other reactions to be rejected.

3. Efficiency Corrections

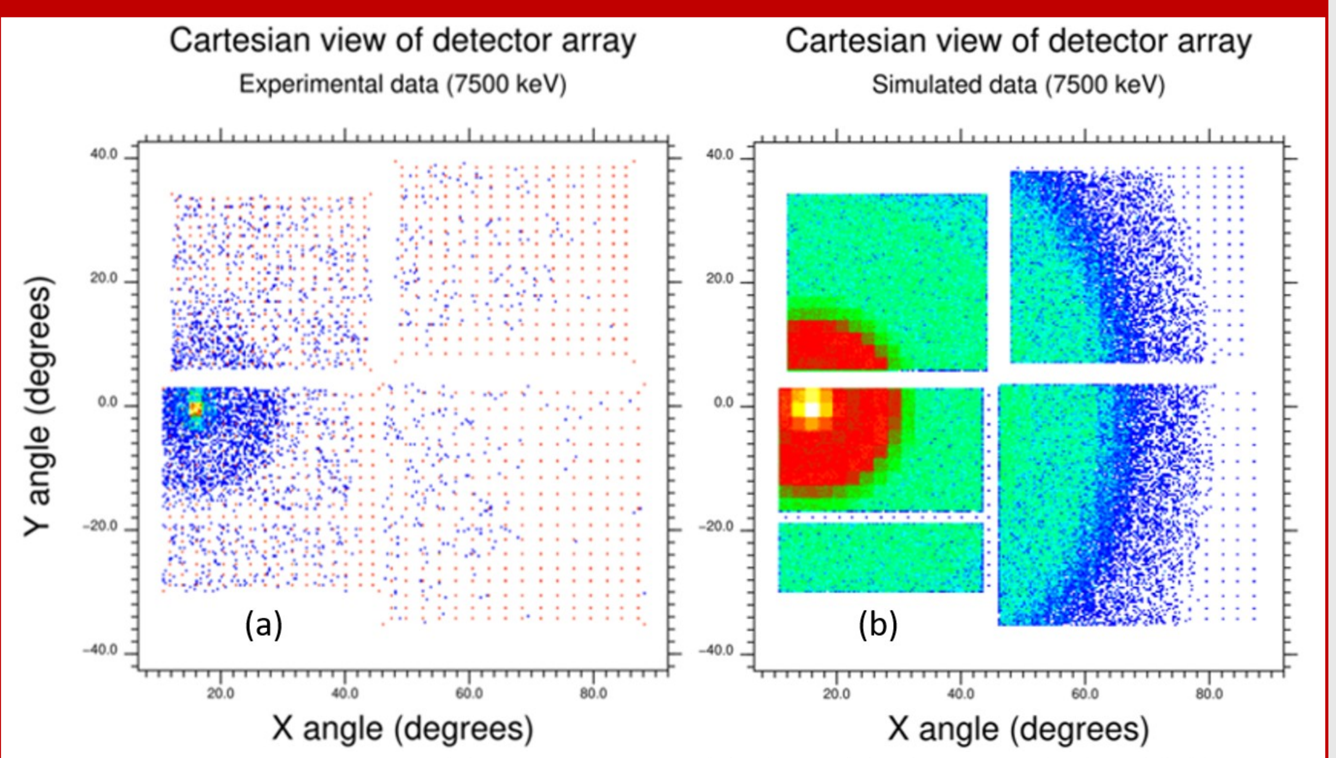

Figure 3: A comparison of the Cartesian views of the front of the detectors in both real (left) and simulated (right) data, showing the agreement in the Gaussian profiles [2].

- In order to accurately determine branching ratios, the **geometric efficiency of the DSSD array for each decay mode** must be considered.
- Through the use of Monte Carlo simulations via Resolution8.1 [5], an in-house simulation package at the University of Birmingham, these geometric efficiencies were determined by **comparing events on each pixel** of the detector to **within 3mm horizontally and vertically**.
- Through measurement of the efficiencies of **bound states**, the geometric efficiencies of the detectors can also be determined.

4. Particle Identification

- The **focal plane detector** of length 0.89 m consists of **2 cathode foils**, **2 anode wires** placed parallel between the two foils and a **scintillator detector** [4].
- One **cathode foil** is segmented into **255 strips** which allowed for a **position measurement** of incoming protons, proportional to their energy.
- The other **cathode foil** and **anode wires** measured **energy loss** of the incident proton, while the **scintillator** measured its **total energy**, enabling **E-ΔE particle identification**.

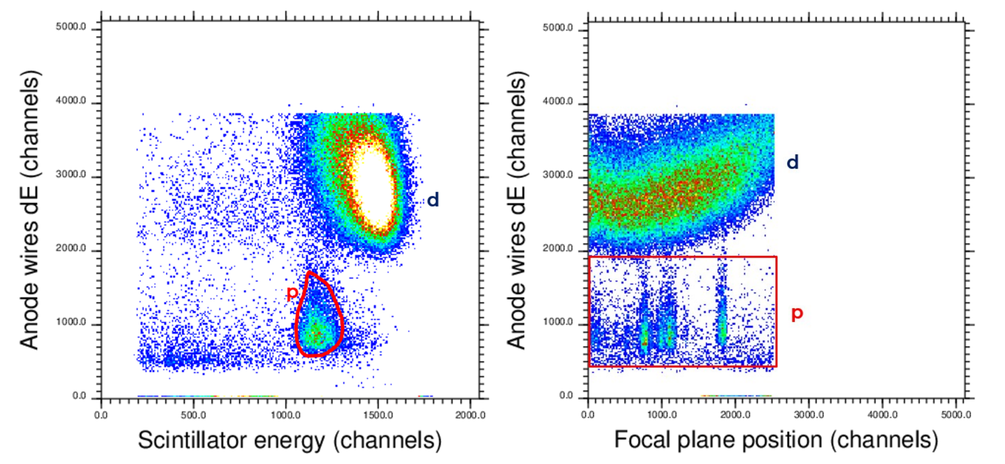

Figure 4: Examples of the focal plane detector particle identification using E-ΔE (left) and using ΔE against focal plane position (right). States in ^{18}O can be seen clearly.

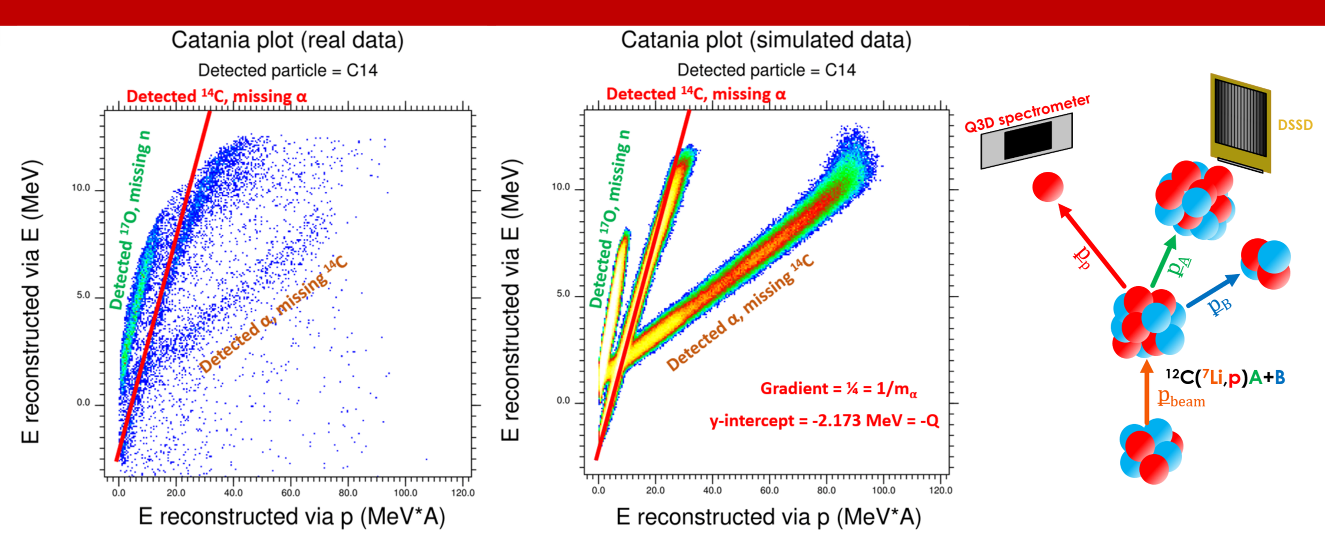

Figure 5: A comparison of Catania plots generated using real (left) and simulated (middle) data assuming a detected ^{14}C, with the different loci labelled [2]. An example reaction is also shown (right).

- As the DSSD array had no inherent particle identification, the nature of a detected particle was determined through **Catania plots**.
- If ^{18}O decays into two massive particles (Figure 5), by assuming the mass of a detected particle (A), the momenta of the other decay fragment (B) can be determined through conservation of momentum.
- By **rearranging the Q-value expression** for this reaction, a relationship in the form **$y = mx + c$** can be obtained,

$$E_{beam} - E_P - E_A = \frac{p_B^2}{2m_B} - Q.$$

- By plotting the left hand side of the equation against $p_B^2/2$, a **straight line locus** formed with a **gradient of $1/m_B$** and a **y-intercept of –Q**.
- As the mass of particle A had to be assumed, there were **distinct loci** associated with the **incorrect assignment of mass**, the nature of which were **confirmed by Monte Carlo simulation**.

5. Preliminary Results

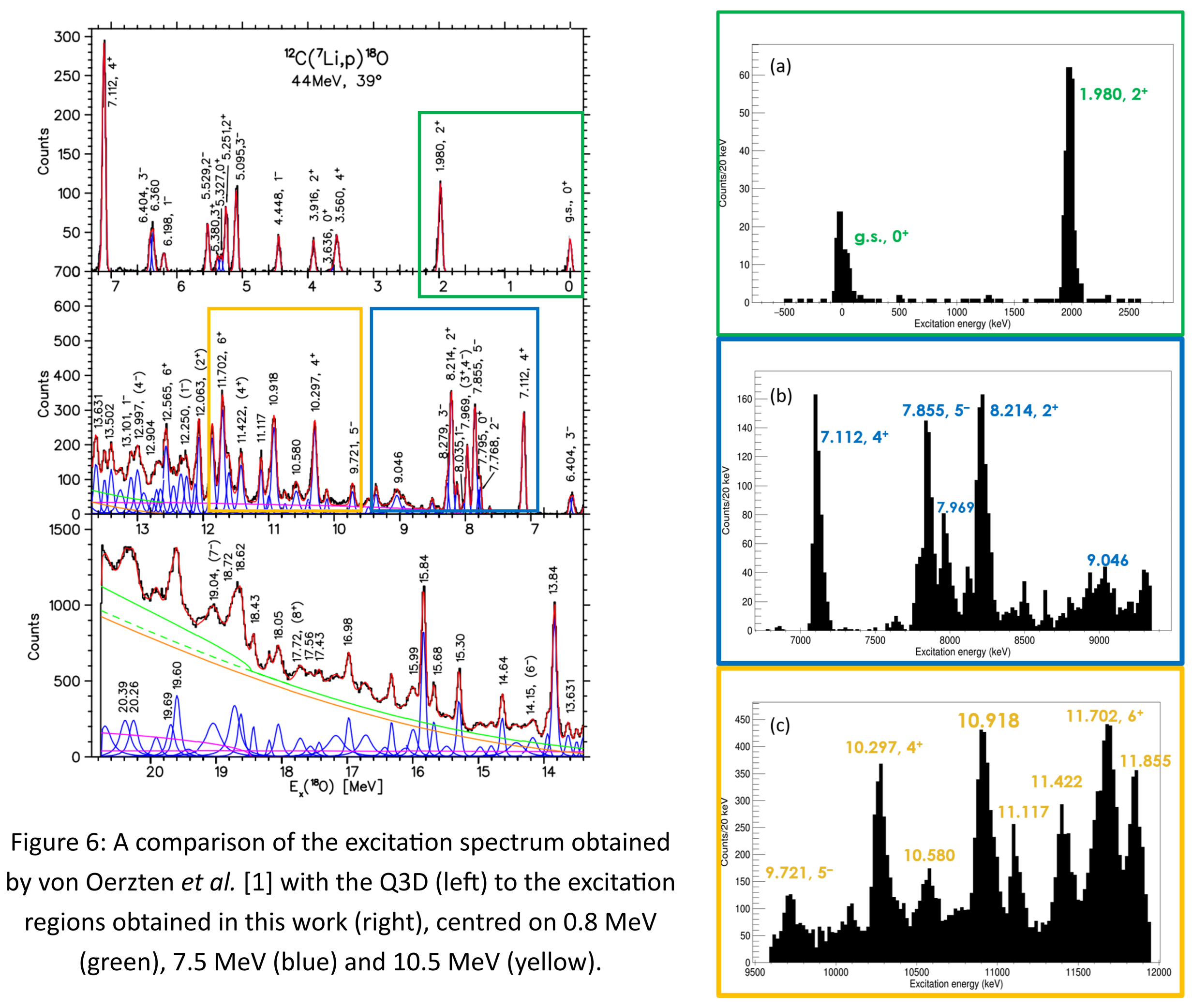

Figure 6: A comparison of the excitation spectrum obtained by von Oertzen *et al.* [1] with the Q3D (left) to the excitation regions obtained in this work (right), centred on 0.8 MeV (green), 7.5 MeV (blue) and 10.5 MeV (yellow).

Table 1: Preliminary branching ratio results obtained for states in the 7.5 MeV excitation region, including their fitted energies and FWHMs, as well as literature J^π values.

Energy (keV)	FWHM (keV)	J^π_{Lit}	α branching ratio	γ branching ratio	^{1}n branching ratio
7114(1)	67.4(14)	4^+	0.27(3)	0.73(3)	-
7621(1)	76(8)	1^-	0.99(13)	0.01(13)	-
7859(2)	62(2)	5^-	0.84(5)	0.16(5)	-
7973(2)	78(4)	$3^+/4^-$	0.04(5)	0.96(5)	-
8127(3)	45(3)	2^+	0.87(9)	0.13(9)	0.00(9)
8411(2)	114.2(12)	1^-	0.00(10)	0.20(10)	0.80(10)

- By **gating on the different loci** on the Catania plot, **the contribution to each state from each decay mode was determined** by fitting the corresponding Q3D spectrum (Figure 7).
- Applying the **geometric efficiency correction** for each decay mode then gave their **absolute branching ratio**.

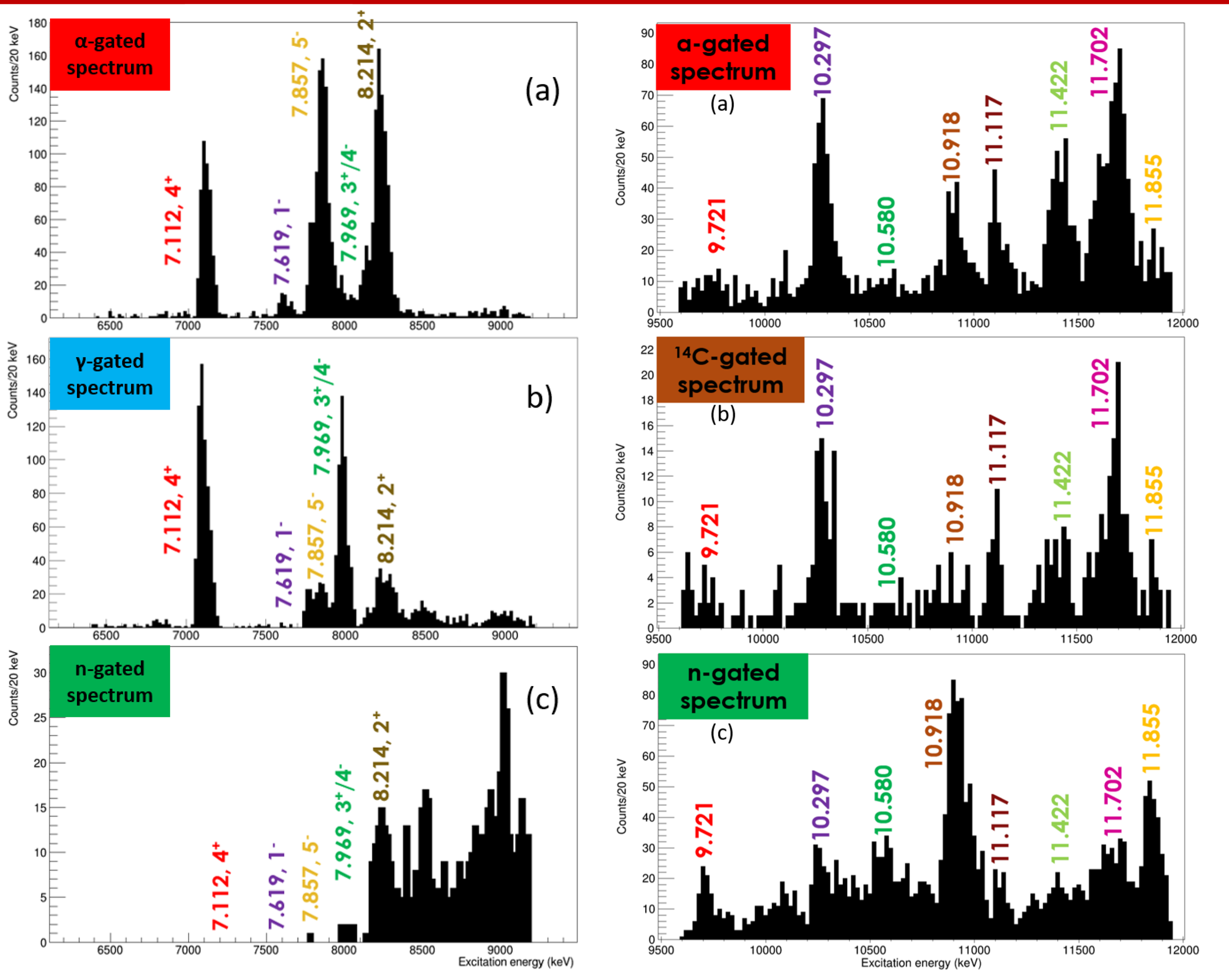

Figure 7: The Q3D spectra obtained for the 7.5 MeV and 10.5 MeV excitation regions when gated on different decay modes. The relative enhancement of states can be seen for each decay mode.

6. Further Work

- Continue extracting **branching ratios** for all measured states.
- Use the measured **branching ratios** to calculate the **reduced partial α widths**.
- Compare the **reduced partial α widths** to the **Wigner limit** and establish the tendency towards α-clustering.

References

1. W. von Oertzen *et al.*, Eur. Phys. J. A, 43:17–33, 2010.
2. S. Pirrie *et al.*, A method to determine γ branching ratios using charged particle detectors for states in ^{18}O, SOTANCP4 conference proceedings, 2018.
3. M. Löffler *et al.*, Nucl. Instrum. Methods, 3:1–12, 1973.
4. H.-F. Wirth, Ph.D. thesis, Technischen Universität, München, 2001.
5. N. Curtis *et al.*, Phys. Rev. C, 51:1554–1557, 1995 .
6. S. Pirrie *et al.*, Phys Rev. C, 2018, paper in preparation.

Acknowledgements

The authors would like to thank Andy Bergmaier for his help loaning equipment during the set-up of the experiment, as well as the operators of the tandem Van de Graaff accelerator at the Maier-Leibnitz Laboratory in Munich for providing and maintaining the ^{7}Li beam. This work was funded by the UK Science and Technology Facilities Council (STFC) under Grant No. ST/L005751/1 and from the European Union's Horizon 2020 research and innovation programme under the Marie Skłodowska-Curie Grant Agreement No. 65F9744.